Journal of Molecular Structure 966 (2010) 129–135

Contents lists available at ScienceDirect

Journal of Molecular Structure

journal homepage: www.elsevier.com/locate/molstruc

The investigation of the interaction between piracetam and bovine serum albumin by spectroscopic methods

Xingjia Guo *, Xiaowei Han, Jian Tong, Chuang Guo, Wenfeng Yang, Jifen Zhu, Bing Fu

College of Chemistry, Liaoning University, Shenyang 110036, PR China

ARTICLE INFO

Article history:
Received 9 November 2009
Received in revised form 10 December 2009
Accepted 14 December 2009
Available online 21 December 2009

Keywords:
Piracetam
Bovine serum albumin
Fluorescence quenching
Circular dichroism
Fourier transform infrared

ABSTRACT

The interaction between piracetam (OPA) with bovine serum albumin (BSA) has been thoroughly studied by fluorescence quenching technique in combination with UV–vis absorption, Fourier transform infrared (FT-IR), and circular dichroism (CD) spectroscopies under the simulative physiological conditions. The quenching of BSA fluorescence by OPA was found to be a static quenching process. The binding constants (K_a) are 3.014, 2.926, and 2.503 $\times$ 10^3 M^{-1} at 292, 298, and 309 K, respectively. According to the van't Hoff equation, the thermodynamic functions standard enthalpy (ΔH) and standard entropy (ΔS) for the reaction were calculated to be -74.560 kJ mol^{-1} and -159.380 J mol^{-1} K^{-1}, which indicated that OPA binds to BSA mainly by hydrogen bonds and van der Waals interactions. The binding distance between BSA and OPA was calculated to be 4.10 nm according to the theory of FÖrster's non-radiation energy transfer. The displacement experiments confirmed that OPA could bind to the site I of BSA. Furthermore, the effects of pH and some common ions on the binding constant were also examined. And the alterations of protein secondary structure in the presence of OPA were observed by the CD and FT-IR spectra.

1. Introduction

Piracetam (2-oxo-1-pyrrolidine acetamide) is a cyclic derivative of gamma-aminobutyric acid. And its molecular structure is shown in Fig. 1. As the most common of the nootropic drugs, OPA is often used in the treatment of patients suffering from pathological neuro sensitive and cognitive deficits, brain-organic psycho syndromes, vertigo and myoclonus of cortical origin. And it can also increase the fluidity of neuronal membrane [1].

Serum albumins are the most abundant proteins in blood. They have many important physiological functions. For instance, they contribute to the osmotic blood pressure and are chiefly responsible for the maintenance of blood pH. But the most important physiological role of albumins involves the binding, transport, and delivery of numerous ligands, such as drugs in the bloodstream to their target organs [2]. Therefore, the investigation of such molecules with respect to albumin binding is of imperative and fundamental importance. Moreover, the studies on the binding of drugs to albumins may provide information of structural features that determine the therapeutic effectivity of drugs, and become an important research field in life sciences, chemistry, and clinical medicine [3–6].

Bovine and human serum albumins display approximately 76% sequence homology, and the 3D structure of BSA is believed to be similar to that of HSA [7]. So the results of all the studies are consistent with the fact that bovine and human serum albumins are homologous proteins. Besides, because of BSA's medical importance, low cost, ready availability, it is often selected as protein model in the related research work [8].

BSA is composed of three linearly arranged, structurally homologous domains (I–III) and each domain in turn is the product of two sub-domains (A, B). It has two tryptophan residues that possess intrinsic fluorescence: Trp-134, which is located on the surface of sub-domain IB, and Trp-212, locating within the hydrophobic binding pocket of sub-domain IIA [8]. The binding sites of BSA for endogenous and exogenous ligands may be in these domains and the principal regions of drugs binding sites of albumin are often located in hydrophobic cavities in sub-domains IIA and IIIA. So called sites I and II are located in sub-domain IIA and IIIA of albumin, respectively. Many ligands bind specifically to serum albumin, for example, ketoprofen in site I [9], flufenamic acid and ibuprofen in site II [10].

Spectroscopic techniques are often applied to reveal the accessibility of quenchers to albumin's fluorophore groups, help understand albumin's binding mechanisms to drugs, and provide clues to nature of binding phenomenon [11].

In the present work, the investigation on the interaction between OPA and BSA was first reported using spectroscopic methods. The binding characteristics between OPA and BSA were analyzed. The binding constants, the binding sites, and the binding distance along with thermodynamic parameters were estimated. In addition, the conformational changes of BSA were explored.

* Corresponding author. Tel.: +86 24 62207809.
E-mail address: guoxja@sina.com (X. Guo).

0022-2860/$ - see front matter © 2009 Elsevier B.V. All rights reserved.
doi:10.1016/j.molstruc.2009.12.025

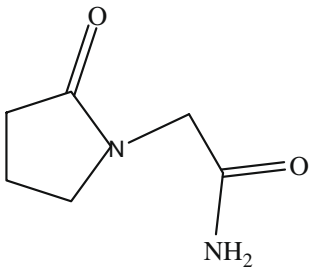

Fig. 1. Molecular structure of piracetam.

2. Experimental

2.1. Materials

The stock solutions of BSA (purity >98%, purchased from Sino-American Biotechnology Company, China) and OPA (provided by Shenyang Watson Pharmaceutical Institute, China) were prepared by dissolving them in water. The stock solutions of ketoprofen and ibuprofen (obtained from the National Institute for Control Pharmaceutical and Products, China) were prepared by dissolving them in a small amount of ethanol, then diluting to the desired concentration with water. All working solutions were prepared in Tris–HCl buffer solution (0.01 M Tris, 0.10 M NaCl, pH 7.43). All chemicals were of analytical reagent grade, and doubly distilled water was used throughout all the experiments.

2.2. Apparatus

Steady state fluorescence measurements were carried out through a Cary Eclipse 300 FL spectrophotometer (Varian Company, USA) equipped with a thermostat bath and 1.0 cm quartz cells, and the excitation and emission slits were set at 5 nm while the scanning rate was 1200 nm min^{-1}; the absorbance measurements were performed on a Cary 5000 UV–vis spectrophotometer (Varian Company, USA) equipped with 1.0 cm quartz cells; the CD measurements were performed on a JASCO-J-810 spectropolarimeter (JASCO, Japan) using a 0.1 cm quartz cell; the FT-IR measurements were carried out on a Nicolet Nexus 670 FT-IR spectrometer (Thermo Nicolet Company, USA) equipped with a Germanium attenuated total reflection (ATR) accessory, a deuterated triglycine sulphate (DTGS) detector and a KBr beam splitter.

2.3. Spectroscopic measurements

All solutions must be rested at least 10 min before the spectrum measurements. Appropriate blanks corresponding to the buffer were subtracted to correct the fluorescence or absorption background.

2.3.1. Fluorescence quenching spectra of BSA

The fluorescence measurements were carried out by keeping the concentration of BSA fixed at 2.0×10^{-6} mol^{-1} and that of OPA was varied from 0 to 13.6×10^{-6} mol L^{-1}. The excitation wavelength was 280 nm and the intrinsic fluorescence emission spectra of BSA at 346 nm was monitored at 292, 298 and 309 K, respectively.

2.3.2. UV–visible absorption spectra

The absorption spectra of BSA in the presence of different concentrations of OPA were recorded in the range of 200–500 nm at room temperature. The concentration of BSA was kept at 5.0×10^{-6} mol L^{-1}, while that of OPA was varied from 0 to 7.5×10^{-5} mol L^{-1}.

2.3.3. FT-IR spectra

All the FT-IR spectra were taken via the attenuated total reflection (ATR) method with a resolution of 4 cm^{-1} and 60 scans at room temperature. The background (containing all system components except protein) were collected at the same condition and subtracted from the spectra of sample solution to obtain the FT-IR spectra of protein. The subtraction criterion was that the original spectrum of protein solution between 2200 and 1800 cm^{-1} was featureless [12].

2.3.4. CD spectra

The CD spectra of BSA (2.0×10^{-6} mol L^{-1}) in the presence of OPA were recorded in the range of 190–250 nm at room temperature under constant nitrogen flush. The molar ratio of OPA to BSA was varied as 0:1, 10:1 and 20:1. And each CD spectrum was obtained using a 0.1 cm cell with at 0.1 nm intervals with three scans.

2.3.5. Displacement experiments

The displacement experiments were performed using the site probes *viz*., warfarin and ibuprofen by keeping the concentration of BSA and OPA constant. And the ratio of OPA to BSA in the BSA + OPA mixture solution was kept at 5:1 in order to keep non-specific binding of probes to a minimum. Then the fluorescence spectra of this mixture solution upon addition of ibuprofen and ketoprofen were recorded upon excitation at 280 nm, respectively.

2.3.6. Effects of common ions and pH

The fluorescence spectra of BSA were recorded upon addition of different concentrations of OPA in the presence of some acid radicals and metal ions *viz*., $C_2O_4^{2-}$, CO_3^{2-}, SO_4^{2-}, PO_4^{3-}, Cu^{2+}, Zn^{2+}, Ca^{2+}, and Mg^{2+} upon excitation at 280 nm. The concentrations of BSA and the common ions were kept constant in the measurement.

The fluorescence spectra of BSA solution titrated by OPA were recorded at pH 6.73, 7.43, and 8.00 upon excitation at 280 nm, respectively.

3. Results and discussions

3.1. Analysis of fluorescence quenching of BSA by OPA

At the excitation wavelength of 280 nm, the fluorescence spectra of BSA with varying concentrations of OPA are shown in Fig. 2. The fluorescence of BSA regularly decreased with the increasing concentration of OPA, but no significant shift of the emission maximum wavelength was observed, indicating that OPA interacted with BSA and quenched its intrinsic fluorescence.

Fluorescence quenching is the decrease of the quantum yield of fluorescence from a fluorophore induced by a variety of molecular interactions with quencher molecule. Under the conditions of fixed pH, temperature and ionic strength, fluorescence quenching may result from ground complex formation, energy transfer and dynamic quenching processes [13]. Dynamic quenching refers to a process that the fluorophore and the quencher come into contact during the lifetime of the excited state, whereas static quenching refers to fluorophore–quencher complex formation.

In order to confirm the type of BSA fluorescence quenching, the procedure was assumed to be dynamic quenching. Usually the experimental data are analyzed by the Stern–Volmer equation [14]:

$$\frac{F_0}{F} = 1 + K_{SV}[Q] \quad (1)$$

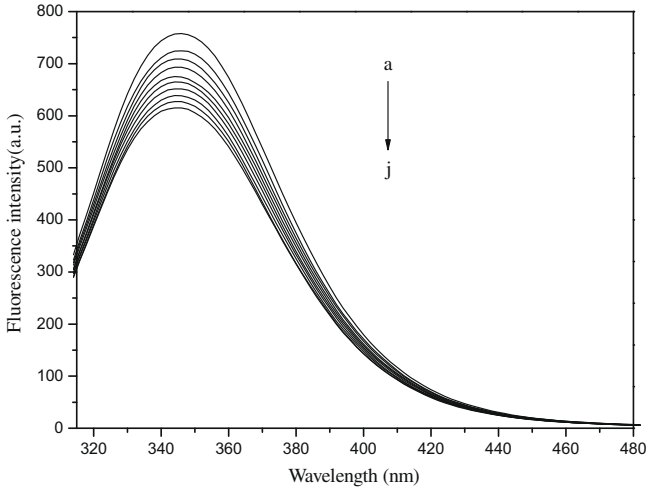

Fig. 2. Fluorescence emission spectra of BSA in the presence of different concentrations of OPA; [BSA] = 2.0 μM; [OPA] = 0.0, 1.7, 3.4, 5.1, 6.8, 8.5, 10.2, 11.9, 13.6 μM, from curve a to j (λ_{ex} = 280 nm, T = 292 K, pH 7.43).

where F_0 and F are the fluorescence intensities in the absence and presence of quencher, respectively. [Q] is the concentration of quencher, and K_{SV} is the Stern–Volmer quenching constant.

Based on the measured fluorescence data at 292, 298, and 309 K, the plots of F_0/F against [OPA] were drawn (Fig. 3), the corresponding the Stern–Volmer quenching constant K_{SV} and the correlation coefficient R^2 was listed in Table 1.

One way to distinguish static quenching from dynamic quenching is to examine their differing dependence on temperature [15]. Dynamic quenching depends upon diffusion: higher temperatures result in larger diffusion coefficients. As a result, the bimolecular quenching constants are expected to increase with temperature rising. In contrast, increased temperature is likely to result in decreasing stability of complexes, and thus lower values of the static quenching constants. Fig. 3 shows that each plot exhibits a good linear relationship and the slope of the Stern–Volmer plot decreases with the temperature rising. Therefore, the possible main quenching mechanism of fluorescence of BSA by OPA should be a static quenching process.

The static quenching equation can be described by so called the Lineweaver–Burk equation [16]

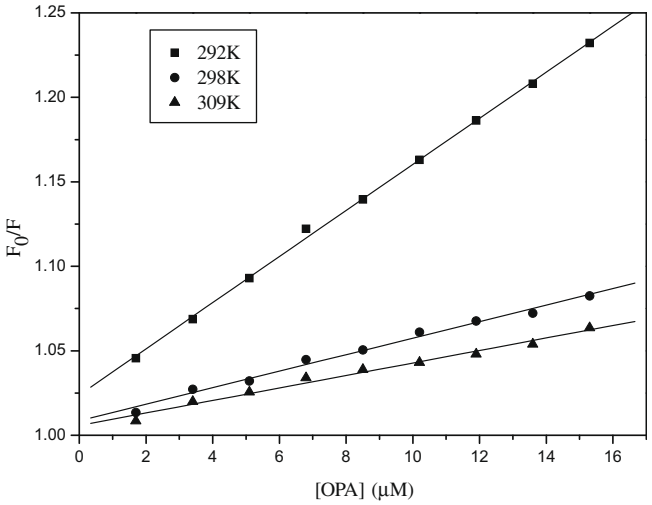

Fig. 3. The Stern–Volmer plots for the quenching of BSA by OPA at different temperatures.

$$(F_0 - F)^{-1} = F_0^{-1} + K_{LB}^{-1}[Q]^{-1}$$

where K_{LB} is the static quenching constant, which can be determined by the slope of the Lineweaver–Burk curves ($(F_0 - F)^{-1}$ versus $[Q]^{-1}$).

The curves of Lineweaver–Burk equation were drawn based on the experimental data of OPA–BSA system at 292, 298, and 309 K, the values of K_{LB} were obtained from the intercept and slope of the curves and listed in Table 1.

3.2. UV–visible absorption spectra

UV–vis absorption measurement is a very simple method and applicable to explore the structural change and know the complex formation [17]. The absorption spectra of BSA in the presence and absence of OPA were recorded and presented in Fig. 4. It is clear from the figure that with the addition of OPA, the absorbance peak around 278 nm which mainly caused by the transition $\pi \rightarrow \pi^*$ of aromatic amino acid residues in BSA are raised [18], indicating BSA molecules binding OPA molecules to form the OPA–BSA complexes. This result reconfirms that the mechanism of fluorescence quenching in OPA–BSA system is a static quenching process.

3.3. Binding constants and binding points

When small molecules bind independently to a set of equivalent sites on a macromolecule, the equilibrium between free and bound molecules is given by the following equation [19]:

$$\log\left(\frac{F_0 - F}{F}\right) = \log K_a + n\log[Q] \quad (2)$$

where in the present case, K_a and n are the binding constant and the number of binding site, respectively. According to Eq. (2), the binding parameters can be obtained by a plot of $\log(\frac{F_0-F}{F})$ versus log[Q].

According to the measured fluorescence data at different temperatures, the fitted plots of $\log(\frac{F_0-F}{F})$ versus log[OPA] were obtained (Fig. 5). The values of K_a and n were calculated from the values of intercept and slope of the plots, respectively, and the results were listed in Table 2. Table 2 shows that K_a decreases slightly with the temperatures rising, but n is approximately equal to 1, indicating that OPA and BSA formed the mol ratio 1:1 complex and the complex would be partly decomposed with the temperature rising.

3.4. Thermodynamic parameters and nature of the binding forces

The interaction forces between quencher and biomolecules may include hydrophobic force, electrostatic interactions, van der Waals interactions, hydrogen bonds, etc. [4]. In order to elucidate the interaction of OPA with BSA, the thermodynamic parameters were calculated. If the enthalpy change (ΔH) does not vary significantly over the temperature range studied, then its value and that of ΔS can be determined from the van't Hoff equation:

$$\ln K = -\frac{\Delta H}{RT} + \frac{\Delta S}{R}$$

where ΔS is the entropy change; K is the Lineweaver–Burk static quenching constant at corresponding temperature; and R is the gas constant.

In the OPA–BSA system, the enthalpy change (ΔH) and the entropy change (ΔS) were obtained from the slope and intercept of the fitted curve of $\ln K_{LB}$ against $1/T$ (Fig. 6), respectively. Then the free energy change (ΔG) was estimated from the following relationship: $\Delta G = \Delta H - T\Delta S$. The values of ΔH, ΔS and ΔG were listed in Table 1. The negative values of ΔG, ΔS and ΔH mean that the binding process is spontaneous and the formation of OPA–BSA

Table 1
The static quenching constants and thermodynamic parameters of OPA–BSA system at different temperatures.

pH	T (K)	K_{LB} ($\times 10^4$ M^{-1})	R^2 (kJ mol^{-1})	ΔH (kJ mol^{-1})	ΔS (J mol^{-1} K^{-1})	ΔG (kJ mol^{-1})
7.43	292	11.71	0.9880	−74.560	−159.380	−22.324
	298	5.34	0.9971			−26.406
	309	1.93	0.9938			−25.465

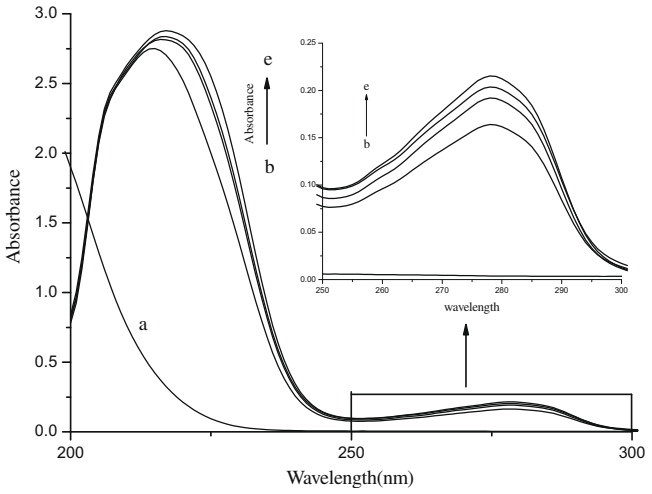

Fig. 4. Absorption spectra of BSA in the presence of OPA. [BSA] = 5.0 μM; [OPA] = 0, 25, 50, 75 μM, from cure b to e; (a) the absorption spectrum of OPA only.

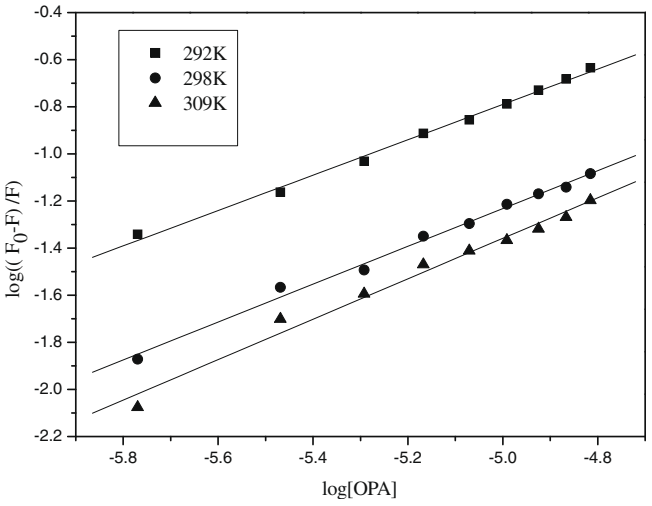

Fig. 5. Polts of $\log(F_0 - F)/F$ versus log[OPA].

Table 2
The binding constants K_a and binding sites n at different temperatures for OPA–BSA system.

T (K)	K_a ($\times 10^3$ M^{-1})	n	R^2
292	3.014	0.7509	0.9976
298	2.926	0.8033	0.9964
309	2.503	0.8475	0.9883

complex is a exothermic reaction. So it was observed in the OPA–BSA system that the binding constant K_a decreased with temperature rising. Moreover, the negative values of ΔS and ΔH suggest that the binding is mainly enthalpy driven and the entropy is unfavorable for it, hydrogen bonds and van der Waals interactions played major roles in the reaction [20].

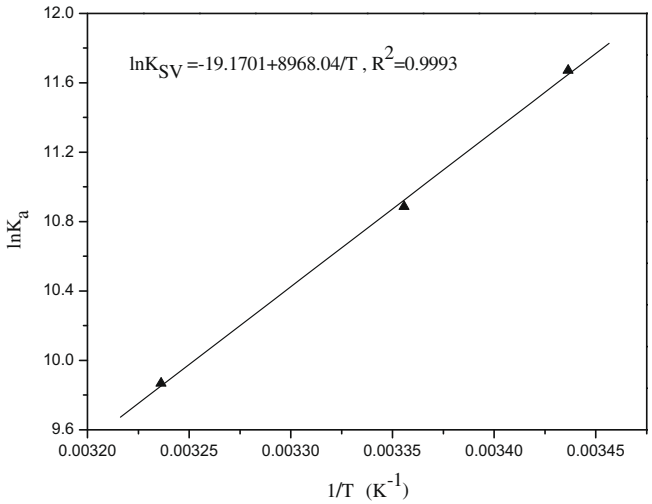

Fig. 6. van't Hoff plot for the interaction of BSA and OPA.

From the molecular structure of OPA shown in Fig. 1, the N—H···O hydrogen bond is easily formed between NH group in OPA and oxygen atom in C═O bond of aromatic amino acid residues in BSA.

3.5. Energy transfer from BSA to OPA

The overlap of the UV–vis absorption spectrum of OPA with the fluorescence emission spectrum of BSA is shown in Fig. 7. The importance of the energy transfer in biochemistry is that the efficiency of transfer can be used to evaluate the distance between the ligand and the tryptophan residues in the protein. According to the theory of FÖrster non-radiative energy transfer [21], the efficiency of energy transfer mainly depends on the following factors (1) the donor can produce fluorescence, (2) fluorescence emission

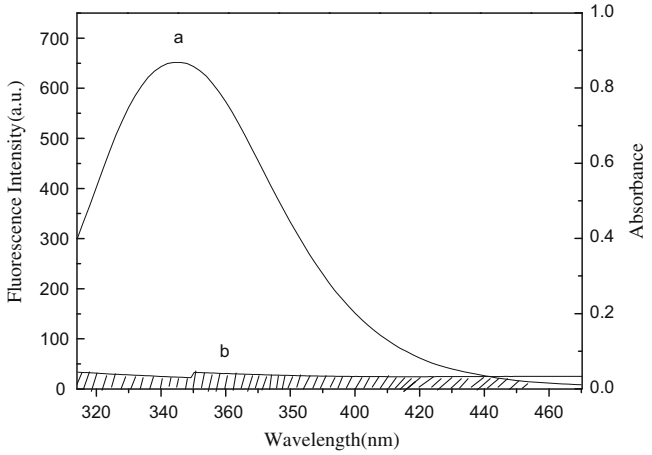

Fig. 7. Overlap of the fluorescence spectrum of BSA (a) and the absorbance spectrum of OPA (b) ([BSA]/[OPA] = 1:1).

spectrum of the donor and UV–vis absorbance spectrum of the acceptor have more overlap and (3) the distance between the donor and the acceptor is approached and lower than 8 nm. The efficiency of energy transfer between the donor and acceptor, E, could be calculated by the following equation:

$$E = 1 - \frac{F}{F_0}\frac{R_0^6}{(R_0^6 + r^6)} \quad (3)$$

where E denotes the efficiency of energy transfer between the donor and the acceptor, and R_0 is the critical distance when the efficiency of energy transfer is 50%. The value of R_0^6 can be calculated using the equation:

$$R_0^6 = 8.8 \times 10^{-25}(JK^2\varphi n^{-4}) \quad (4)$$

where K^2 is the spatial orientation factor related to the geometry of the donor and acceptor of dipoles, and $K^2 = 2/3$ for random orientation as in fluid solution; n is the averaged refracted index of the medium in the wavelength range where spectral overlap is significant; φ is the fluorescence quantum yield of the donor; and J is the spectral overlap integral between the fluorescence emission spectrum of the donor and the absorption spectrum of the acceptor. The value of J can be calculated by the equation:

$$J = \frac{\int_\infty F(\lambda)\varepsilon(\lambda)\lambda^4 d\lambda}{\int_0^\infty F(\lambda)d\lambda} \quad (5)$$

where $F(\lambda)$ is the corrected fluorescence intensity of the donor in the wavelength range from λ to $\lambda + \Delta\lambda$; $\varepsilon(\lambda)$ is the molar absorption coefficient of the acceptor at wavelength λ. In the present case, $n = 1.36$ and $\varphi = 0.15$ [2]. From Eqs. (3)–(5), $J = 3.03 \times 10^{-14}$ cm^3 L mol^{-1}, $E = 0.14$, $R_0 = 3.03$ nm, and $r = 4.10$ nm were calculated. As the binding distance $r = 4.10$ nm is less than 8 nm, and $0.5R_0 < r < 1.5R_0$, the energy transfer from BSA to OPA occurred with high possibility [22].

3.6. The displacement experiments of site probes

BSA has a large hydrophobic cavity that can accommodate two or more ligands. When two ligands (denoted with L_1 and L_2) bind to BSA simultaneously, two types of interaction can occur [23]:

(1) competitive binding

$$L_1 \overset{+BSA}{\rightarrow} L_1 - BSA \overset{+L_2}{\rightarrow} L_2 - BSA + L_1$$

(2) non-competitive binding

$$L_1 \overset{+BSA}{\rightarrow} L_1 - BSA \overset{+L_2}{\rightarrow} L_2 + BSA - L_1$$

In order to identify the location of the OPA binding site on BSA, the displacement experiments were carried out using the site probes ibuprofen and ketoprofen. The percentage of fluorescence probe displaced by the drug was determined by measuring the changes in fluorescence intensity according to the method proposed by Sudlow et al. [24]:

$$F_2/F_1 \times 100\%$$

where F_1 and F_2 denote the fluorescence of drug plus protein without the probe and with the probe, respectively.

Based on the spectral data measured in the displacement experiment, the plots of F_2/F_1 against site probe concentration were fitted (Fig. 8). It could be seen from this figure that the fluorescence of BSA was remarkably affected by adding ketoprofen, conversely the addition of ibuprofen to the same solution. These results indicate that ketoprofen displaced OPA from the binding site while ibuprofen had a little effect on the binding of OPA to BSA. Hence, it can be concluded that OPA was bound to site I in sub-domain IIA of BSA, namely Trp-212 is near or within the OPA binding site.

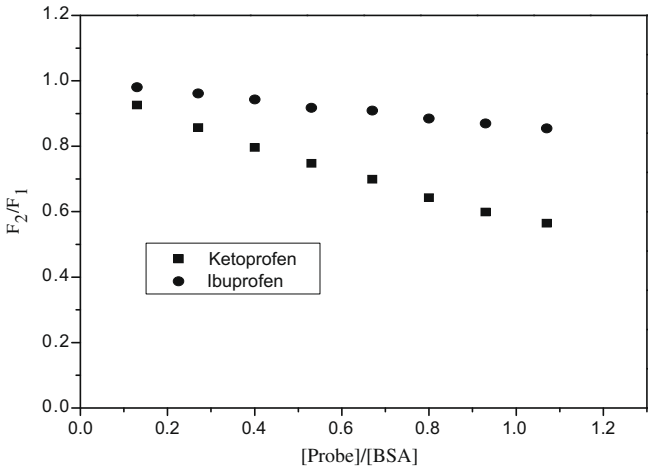

Fig. 8. Effect of site marker probes on the fluorescence of OPA–BSA; [BSA] = 10 μM.

3.7. Effects of common ions on the binding constants of the OPA–BSA complex

There exist some anions and metal ions in the blood system. These ions not only play many physiological roles, such as buffer action and maintenance of osmotic pressure, but also can directly influence the binding force of drug with protein. In this paper, the effect of some common ions $C_2O_4^{2-}$, SO_4^{2-}, CO_3^{2-}, PO_4^{3-}, Cu^{2+}, Zn^{2+}, Ca^{2+}, and Mg^{2+} on the binding constant of OPA–BSA complex was investigated. The results were listed in Table 3. Except Cu^{2+} and Ca^{2+}, the competition between OPA and the other ions made the binding constant of OPA–BSA complex decrease compared to the binding constant without these ions. Although these ions and OPA are likely to bind at different sites in BSA, they still restrain the binding reaction between OPA and BSA [25]. Consequently, the binding affinities of drug to protein can be weakened. The reason why the binding constant of OPA–BSA complex increased in the presence of Cu^{2+} and Ca^{2+} can be explained as follows: Cu^{2+} and Ca^{2+} induced the conformational changes of albumins, which is more favorable for OPA binding to BSA; or the metal ion–OPA complexes were formed via metal ion bridges [26], which more easily bind with protein. In a word, the presence of common ions may shorten or prolong the storage time of OPA in blood plasma and enhance or weaken its maximum effects.

3.8. Effect of pH

The binding of OPA with BSA was also studied at three different pH values (6.73, 7.43 and 8.00). Binding constants are given in Table 4. These data shows a decrease in the binding constants on decreasing the pH from 7.43 to 6.73 or increasing from 8.0 to 7.43. Because both of OPA and BSA carry negatively charged at

Table 3
The effects of coexisting metal ions on the binding constant of OPA–BSA system.

System	K_a (ions)/K_a (without ions)	R^2
BSA–OPA + Cu^{2+}	1.117	0.9962
BSA–OPA + Ca^{2+}	1.126	0.9950
BSA–OPA + Zn^{2+}	0.874	0.9911
BSA–OPA + Mg^{2+}	0.853	0.9933
BSA–OPA + PO_4^{3-}	0.858	0.9980
BSA–OPA + CO_3^{2-}	0.656	0.9970
BSA–OPA + SO_4^{2-}	0.599	0.9827
BSA–OPA+$C_2O_4^{2-}$	0.486	0.9920

pH 6.73, the electrostatic repulsion may be responsible for the decrease in the binding capacity. And the increase of binding constant with pH from 7.43 to 8.00 should be attributed to the N—B transition in albumin [27]. Thereby, it can be elicited that the binding reaction of OPA and protein in plasma is sensitive to the change in pH, and the pH 7.43 is the optimal acidity.

3.9. FT-IR spectra

Infrared spectra of proteins exhibit a number of amide bands, which represent different vibrations of peptide moieties. Among the amide bands of the protein, amide I band (mainly C=O stretch) and amide II band (C—N stretch coupled with N—H bending mode) have been widely used as the typical ones. They both have relationship with the secondary structure of the protein. However, the amide I band is more sensitive to the change of protein secondary structure than amide II [28].

To explore the changes of the BSA secondary structure after OPA bound to BSA, the FT-IR spectra of BSA were recorded. The FT-IR spectra and difference spectra of BSA are shown in Fig. 9. After OPA was added, it could be observed that the intensity of amide I band distinctly decreased, but the peak positions of amide I and amide II bands had no significant shift. It was important to note that the decrease in the intensity of amide I band was due to the decrease of the proportion of protein α-helix structure [11]. So we concluded that the α-helix content of BSA was reduced upon binding with OPA. It is apparent that the formation of the OPA–BSA complexes caused the rearrangement of the polypeptide carbonyl hydrogen bonding network and finally the reduction of the α-helical structure of proteins. Therefore, the secondary structures of BSA were changed by the interaction of OPA with BSA.

3.10. CD spectra

To further investigate whether any conformational changes of BSA molecules occurred in the binding reaction, the measurement of CD spectra was performed. The CD spectra of BSA in the absence and presence of OPA are shown in Fig. 10. In this experiment, in order to observe apparent change of protein CD spectra, more OPA was added into BSA solutions. With the increasing addition of OPA, the band intensity of curves (a → c) decreased regularly. And there exhibited two negative bands in the UV region at 208 and 222 nm, characteristic of an α-helical structure of protein [15]. However, the CD spectra of BSA in the absence and the presence of OPA are similar in shape, indicating that the structure of BSA after the addition of OPA is also predominantly α-helix. The CD results are expressed in terms of mean residue ellipticity (MRE) in deg cm^2 dmol^{-1} according to the following equation [29]:

$$\mathrm{MRE} = \frac{\text{Observed CD (medg)}}{C_p n l \times 10} \tag{6}$$

where C_p is the molar concentration of the protein, n the number of amino acid residues and l is the path length. The α-helical contents of free and combined BSA were calculated from MRE values at 208 nm using the equation [29]:

$$\alpha\text{-Helical } (\%) = \frac{-\mathrm{MRE}_{208} - 4000}{33,000 - 40,000} \times 100 \tag{7}$$

where MRE_{208} is the observed MRE value at 208 nm, 4000 is the MRE of the β-form and random coil conformation cross at 208 nm and 33,000 is the MRE value of a pure α-helix at 208 nm. From Eqs. (6) and (7), the α-helicity in the secondary structure of BSA were calculated to be 47% in free BSA, 44.5% and 41.8% in the OPA–BSA complex with the molar ratios of OPA to BSA 10:1 and 20:1, respectively. The decrease of α-helix percentage indicated that the binding of OPA to the amino acid residues of main polypeptide chain of protein and then the hydrogen bonding networks of the protein was destroyed [30], namely the binding of OPA and BSA induced some secondary-structure changes in BSA.

Table 4
Effect of pH on the binding constant of OPA–BSA complex.

pH	K_a ($\times 10^3$ M^{-1})	R^2
6.73	2.2417	0.9974
7.43	2.2978	0.9934
8.00	0.8879	0.9972

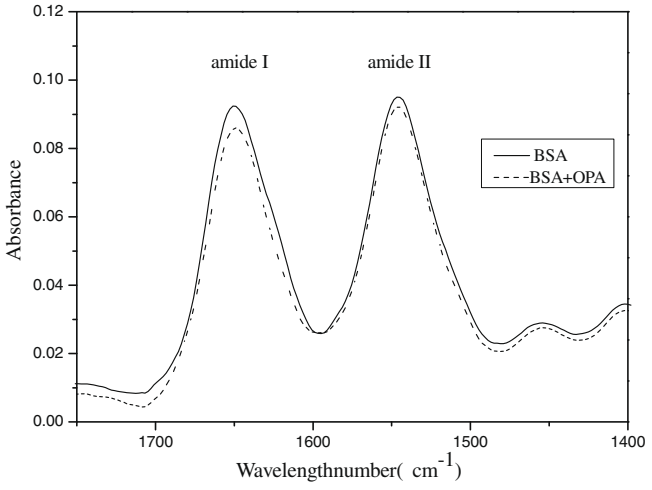

Fig. 9. FT-IR spectra of free BSA and difference spectra of OPA + BSA [(OPA + BSA solution) − (OPA solution)] in the region of 1750–1400 cm^{-1}; [OPA] = 25 μM; [BSA] = 500 μM.

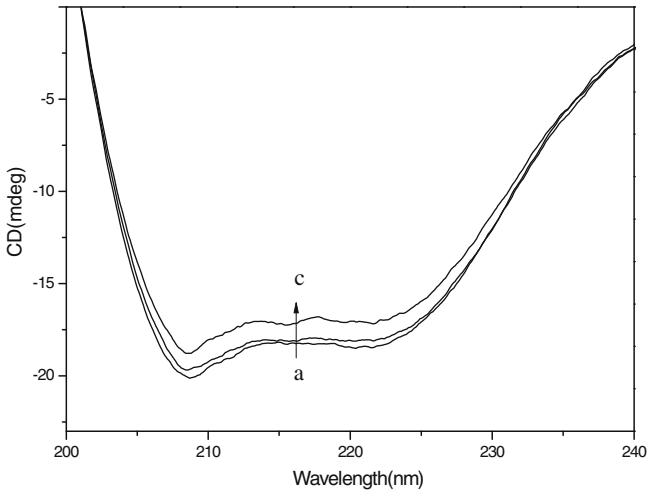

Fig. 10. CD spectra of BSA at pH 7.43 as a function of OPA concentration. (a) 0:1; (b) 10:1; (c) 20:1 (the ratio in this figure is the concentration ratio of OPA to BSA).

4. Conclusions

In this paper, the interaction of OPA with BSA has been investigated by spectroscopic techniques. The fluorescence quenching results show that the probable quenching mechanism of fluorescence of BSA initiated by OPA is a static quenching process. The results also reveal the presence of a single class of binding site with a relatively small binding constant and a complex formation at 1:1 mol ratio in OPA–BSA system; and hydrogen bonds and van der Waals interactions played major roles in stabilizing the

complex. The value of the distance r indicates that the energy transfer from BSA to OPA occurred. Analysis of CD and FT-IR spectra indicates that the formation of OPA–BSA complex induced changes in the secondary structure of protein with a small reduction in the α-helix content. The displacement experiment shows that OPA was located in sub-domain IIA (site I) of BSA.

The binding study of drugs with albumins is of great importance in pharmacy, pharmacology and biochemistry. This study is expected to provide some significative clues to clinical research and the theoretical basis for pharmacology.

Acknowledgement

We gratefully acknowledge financial support of Education Foundation of Liaoning Province, China (Grant No. 20060362).

References

[1] A. Curticapean, S. Imre, J. Biochem. Biophys. Methods 69 (2007) 273–281.
[2] R.E. Olson, D.D. Christ, Annu. Rep. Med. Chem. 31 (1996) 327–337.
[3] P.B. Kandagal, S. Ashoka, J. Seetharmappa, J. Pharm. Biomed. 41 (2006) 393–399.
[4] Y.N. Ni, G.L. Liu, S. Kokot, Talanta 76 (2008) 513–521.
[5] A.R. Timerbaev, C.G. Hartinger, S.S. Aleksenko, Chem. Rev. 106 (2006) 2224–2248.
[6] P.L. Gentili, F. Ortica, G. Favaro, J. Phys. Chem. B 112 (2008) 16793–16801.
[7] C. Leslie, C.J.W. Scott, F.I. Cair, Med. Lab. Sci. 49 (1992) 319–325.
[8] V. Anbazhagan, R. Renganathan, J. Lumin. 128 (2008) 1454–1458.
[9] X.M. He, D.C. Carter, Nature 358 (1992) 209–215.
[10] I. Sjoholm, B. Ekman, A. Kober, Mol. Pharmacol. 16 (1979) 767–777.
[11] Y.Y. Yue, Y.H. Zhang, L. Zhou, J. Qin, X.G. Chen, J. Photochem. Photobiol. B 90 (2008) 26–32.
[12] A.C. Dong, P. Huang, W.S. Caughey, Biochemistry 29 (1990) 3303–3308.
[13] M. Bhattacharyya, U. Chaudhuri, R.K. Poddar, Biochem. Biophys. Res. Commun. 167 (1990) 1146–1153.
[14] J.R. Lakowicz, Principles of Fluorescence Spectroscopy, second ed., Plenum Press, New York, 1999. pp. 237–265.
[15] X.J. Guo, L. Zhang, X.D. Sun, X.W. Han, C. Guo, P.L. Kang, J. Mol. Struct. 928 (2009) 114–120.
[16] F.L. Cui, Q.Z. Zhang, X.J. Yao, H.X. Luo, Y. Yang, Pestic. Biochem. Physiol. 90 (2008) 126–134.
[17] S. Ashoka, J. Seetharamappa, P.B. Kandagal, S.M.T. Shaikh, J. Lumin. 121 (2006) 179–186.
[18] Y.Q. Wang, B.P. Tang, H.M. Zhang, J. Photochem. Photobiol. B 94 (2009) 183–190.
[19] C. Wang, Q.H. Wu, Z. Wang, J. Zhao, Anal. Sci. 22 (2006) 435–438.
[20] P.D. Ross, S. Subramanian, Biochemistry 20 (1981) 3096–3120.
[21] T. FÖrster, O. Sinanoglu (Eds.), Modern Quantum Chemistry, vol. 3, Academic Press, New York, 1966. p. 93.
[22] B. Valeur, J.C. Brochon, New Trends in Fluorescence Spectroscopy, sixth ed., Springer Press, Berlin, 1999. pp. 25–28.
[23] Y.N. Ni, X. Zhang, S. Kokot, Spectrochim. Acta A 71 (2009) 1865–1872.
[24] G. Sudlow, D.J. Birkett, D.N. Wade, Mol. Pharmacol. 12 (1976) 1052–1061.
[25] N. Wang, L. Ye, F.F. Yan, R. Xu, Int. J. Pharm. 351 (2008) 55–60.
[26] J.B. Xiao, J. Shi, H. Cao, S.D. Wu, F.L. Ren, M. Xu, J. Pharm. Biomed. Anal. 45 (2007) 609–615.
[27] W.F. van der Giesen, Biochem. Pharmacol. 32 (1983) 281–285.
[28] K.S. Witold, H.M. Henry, C. Dennis, Biochemistry 32 (1993) 389–394.
[29] G. Hong, L. Liandi, L. Jiaqin, Q. Kong, C. Xingguo, Z. Hu, J. Photochem. Photobiol. A 167 (2004) 213–221.
[30] Y.Z. Zhang, J. Dai, X.P. Zhang, X. Yang, Y. Liu, J. Mol. Struct. 888 (2008) 152–159.